Published in final edited form as:
Biol Psychiatry. 2013 March 1; 73(5): 443–453. doi:10.1016/j.biopsych.2012.09.026.

Synaptic dysfunction in the hippocampus accompanies learning and memory deficits in HIV-1 Tat transgenic mice

Sylvia Fitting[1], **Bogna M. Ignatowska-Jankowska**[1], **Cecilia Bull**[2], **Robert P. Skoff**[3], **Aron H. Lichtman**[1,4], **Laura E. Wise**[1], **Michael A. Fox**[2], **Jianmin Su**[2], **Alexandre E. Medina**[2], **Thomas E. Krahe**[2], **Pamela E. Knapp**[1,2,4], **William Guido**[2], and **Kurt F. Hauser**[1,4]

[1]Departments of Pharmacology & Toxicology, Virginia Commonwealth University, Medical College of Virginia Campus, Richmond, VA 23289

[2]Anatomy & Neurobiology, Virginia Commonwealth University, Medical College of Virginia Campus, Richmond, VA 23289

[3]Department of Anatomy & Cell Biology, Wayne State University, School of Medicine, Detroit, MI 48202

[4]Institute for Drug and Alcohol Studies, Virginia Commonwealth University, Medical College of Virginia Campus, Richmond, VA 23289

Abstract

Background—Human immunodeficiency virus (HIV) associated neurocognitive disorders (HAND), including memory dysfunction, continue to be a major clinical manifestation of HIV type-1 (HIV-1) infection. Viral proteins released by infected glia are thought to be the principal triggers of inflammation and bystander neuronal injury and death, thereby driving key symptomatology of HAND.

Methods—We used a GFAP-driven, doxycycline (DOX)-inducible HIV-1 Tat (transactivator of transcription) transgenic mouse model and examined structure-function relationships in hippocampal pyramidal CA1 neurons using morphologic (Golgi-silver impregnations, immunohistochemistry, TUNEL detection, *synaptic protein markers,* electron microscopy), electrophysiological (long-term potentiation (LTP)), and behavioral (Morris water maze, fear-conditioning) approaches.

Results—Tat induction caused a variety of different inclusions in astrocytes characteristic of lysosomes, autophagic vacuoles, and lamellar bodies, which were typically present within distal cytoplasmic processes. In pyramidal CA1 neurons, Tat induction reduced the number of apical dendritic spines, while disrupting the distribution of synaptic proteins (synaptotagmin 2 and gephyrin) associated with inhibitory transmission, but with minimal dendritic pathology and no evidence of pyramidal neuron death. Electrophysiological assessment of excitatory postsynaptic field potential (fEPSP) at Schaffer collateral/commissural fiber-CA1 synapses showed near total suppression of LTP in mice expressing Tat. The loss in LTP coincided with disruptions in learning and memory.

Corresponding Author: Sylvia Fitting, Ph.D. Dept. Pharmacology and Toxicology Virginia Commonwealth University Richmond, VA 23298 804-628-7580 (phone) 804-827-9974 (FAX) sfitting@vcu.edu.

Financial Disclosures The authors report no biomedical financial interests or potential conflicts of interest.

Conclusion—Tat expression in the brain results in profound functional changes in synaptic physiology and in behavior that are accompanied by only modest structural changes and minimal pathology. Tat likely contributes to HAND by causing molecular changes that disrupt synaptic organization, with inhibitory presynaptic terminals containing synaptotagmin 2 appearing especially vulnerable.

Keywords

NeuroAIDS; hippocampal area CA1; electron microscopy; synaptotagmin; gephyrin; neuroplasticity; long-term potentiation; Morris water maze; spatial learning; fear conditioning

Introduction

Central nervous system (CNS) function relies on specific pre- and postsynaptic interconnections among neurons [1, 2]. Pathological elimination of synaptic integrity likely contributes to significant behavioral impairment in neurologic disorders. Synaptic dystrophy initiated through damage to the molecular scaffolding of the postsynaptic density, and subsequent spine dystrophy and culling [3-7], are likely to underlie significant neurocognitive impairment [8, 9]. A similar gradual decline in function, accompanied by diminishing connectivity, is seen during a variety of progressive degenerative diseases including Alzheimer's disease [10] and Parkinson's disease [11].

Synaptic and dendritic culling are the best predictors of human immunodeficiency virus (HIV) associated neurocognitive disorders (HAND) [8, 9, 12], which remains amongst the most common disorders in people infected with HIV type-1 (HIV-1) despite potent combination antiretroviral therapy (cART) [13-15]. Sublethal alterations in neuronal circuitry occur early in Alzheimer's disease, years before the onset of clinical symptoms [16]. They have been assumed to occur in HIV, but this has not been rigorously studied ultrastructurally or functionally at the level of the synapse.

While HIV-1 is known to disrupt synaptic machinery and neurocognition, the precise mechanisms are less well understood and attributable to multiple viral and cellular reactive products [17-21]. The molecular actions of HIV-1 toxins, such as glycoprotein 120 (gp120) and transactivator of transcription (Tat), and the destabilizing actions of reactive cellular products, including excitatory amino acids (glutamate and quinolinic acid), reactive oxygen species (ROS), and proinflammatory cytokines [4, 20, 22-24] appear to control critical, but separate, aspects of neuronal damage. Tat is produced very early after infection and is necessary for HIV replication, and thereby driving disease progression [25-31]. Although entry inhibitors, nucleoside and non-nucleoside reverse transcriptase inhibitors block the viral entry and integration, and protease inhibitors block the assembly of *de novo* viral particles, once cells have been infected, cART fails to restrict Tat transcription and translation [32]. Tat is a toxic protein which at high concentrations contributes to neuronal injury via excitotoxic mechanisms [4, 33-40], by overactivating *N*-methyl D-aspartate receptors (NMDARs), causing pathological increases in $[Ca^{2+}]_i$ [41], and triggering caspase-dependent and/or -independent cell death [4, 42]. In contrast, little is known about the effects of chronic, low levels of Tat exposure on CNS function in HIV-1-infected patients. Vaccinations against Tat can enhance cART efficacy and to restore immune homeostasis [31, 43].

Using inducible Tat transgenic mice, we reported that Tat exposure resulted in neuron injury in the striatum without causing neuron death [44]. This agreed with descriptions of synapse elimination unaccompanied by neuron death [7, 45-48], but was contrary to reports of pronounced and precipitous lethality by Tat *in vitro* [19, 49]. By an alternative approach *in*

vitro, Tat impaired network function in hippocampal neurons via the low-density lipoprotein receptor-related protein without decreasing neuronal survival [50]. Here we describe Tat-induced sublethal changes in hippocampal CA1 neuron structure and function that coincide with defects in learning and memory, but in the absence of overt neuronal death. It is hypothesized that Tat is one of the proteins responsible for the sustained CNS complications seen in HIV-1 patients receiving cART. We propose that the chronic Tat transgenic model of HIV-1 mimics key aspects of the true pathophysiologic events underlying HAND in the post-cART era.

Methods and Materials

Animals and doxycycline (DOX) administration

GFAP-driven, DOX-inducible, Tat transgenic male mice were used to evaluate the effects of the Tat protein on hippocampal structure, function and behavior. The generation of DOX-inducible, brain-specific HIV-Tat transgenic mice have been previously reported [44, Supplementary Methods]. Tat expression was induced with a specially formulated chow containing 6 mg/kg DOX (Harlan, Indianapolis, IN), fed to control Tat(−) mice that lack the Tat transgene (Tat−/DOX) and inducible Tat(+) mice (Tat+/DOX) for 1-2 wk [44, 51, Supplementary Methods], except where indicated otherwise. Animal procedures were approved by the Virginia Commonwealth University Institutional Animal Care and Use Committee (IACUC) and conform to AAALAC guidelines.

Assessment of dendritic pathology

Dendritic pathology was assessed in hippocampal tissues (120 μm) of adult (2-3-mo old) Tat−/DOX (n = 6) and Tat+/DOX (n = 6) mice using a modified Golgi-Kopsch procedure [52, 53, Supplementary Methods]. The length and morphology, and the density of spines on the apical dendrites of pyramidal neurons in the stratum radiatum (sr) of CA1, were quantified using established criteria (Supplementary Methods).

Cell death assessment

Neuron death was assessed in hippocampal sections (12 μm) from 2-3-mo-old Tat−/DOX (n = 4) and Tat+/DOX (n = 4) mice labeled for terminal deoxynucleotidyl transferase-mediated UTP nick end-labeling (TUNEL), NeuN, and Hoechst (Supplementary Methods). To assess neuron death, the proportion of cells in which $TUNEL^+$ and $NeuN^+$ was co-detected was determined (Supplementary Methods).

Electron microscopy

The hippocampi from 2-3-mo old Tat−/DOX and Tat+/DOX mice were prepared and processed for transmission electron microscopy (TEM) (Supplementary Methods). Sections were observed with a JEOL JEM-1230 TEM (JEOL USA, Inc.) and images obtained using a Gatan Ultrascan 4000 digital camera (Gatan Inc., Pleasanton, CA).

Assessment of synaptic vesicle-associated proteins

Seven pre- and postsynaptic vesicle-associated protein markers were assessed by western blotting *and immunohistochemistry* in CA1 hippocampal tissues from 3-mo old Tat−/DOX (n = 3) and Tat+/DOX (n = 3) mice (Supplementary Methods). The 5 presynaptic markers included antibodies to (1) synaptotagmin 2 (Syt2) that detects recombinant Syt2 but not Syt1 [54], (2) Synapsin (Syn) that labels nerve terminals in mouse hippocampus [55], (3) glutamate decarboxylase 67 (Gad67) that labels interneurons and inhibitory nerve terminals in the hippocampus [56], and (4 & 5) vesicular glutamate transporters 1 (VGlut1) and 2 (VGlut2). The 2 postsynaptic markers included (1) postsynaptic density protein 95 (PSD-95)

that labels postsynaptic densities, and (2) gephyrin (Geph) that labels postsynaptic structures at inhibitory synapses [57]. Synaptic proteins were normalized to actin levels. Prompted by significant immunoblot findings, possible intraregional differences in Syt2 and gephyrin distribution were assessed by semi-quantitative measures of immunofluorescence intensity in 3-mo old control (Tat−/DOX) (n = 3) and Tat+/DOX mice (n = 3) (Supplementary Methods).

Electrophysiology

Hippocampal slices were prepared from young adult (1-mo old) Tat−/DOX (n = 4, P22-26, 23.5±0.87) and Tat+/DOX (n = 4, P25-27, 26.0±0.41) mice using standard techniques (Supplementary Methods). Recordings were conducted in one slice per animal. The Schaffer collaterals were stimulated and field potentials were recorded in the stratum radiatum of CA1 in slices perfused in ACSF (perfusion rate, 1 ml/min; with 95% O_2, and 5% CO_2 at 30 ± 2°C) using an interface recording chamber. To induce long-term potentiation (LTP), one single train of high-frequency stimulation (HFS) at 100 Hz (100 pulses for 1 s duration) was delivered, using the same stimulation intensity as for baseline stimulation (Supplementary Methods). fEPSP peak data were converted to percentages by setting the baseline fEPSP peak data of the Tat−/DOX mice to 100%.

Morris water maze assessment

The Morris water maze task was used to assess spatial learning and memory in adult (2-3-mo old) Tat−/DOX (n = 9) and Tat+/DOX (n = 9) mice (Supplementary Methods). During acquisition training (5 d), the animal's swimming behavior was recorded for 60 s. Latency (s), distance traveled (cm), and swimming speed (cm/s) were calculated for each trial. The probe test was conducted 2 d after the last acquisition session and mice were allowed to swim freely for 20 s. The average proximity (cm) to the location of the absent target platform was determined for each mouse, while time spent in each of the four quadrants was also calculated (Supplementary Results).

Contextual fear-conditioning assessment

Following a 28 d DOX exposure, adult (3-4 mo old) Tat+/DOX (n = 9) and Tat−/DOX (n = 7) mice were tested in a contextual fear-conditioning paradigm. For conditioning, the mice were placed in the experimental chamber (47.5 × 41 × 22 cm) for 3 min, during which time baseline freezing behavior was measured. At 3 min, each subject received one mild foot shock (2 s, 0.7 mA) and post-shock freezing behavior was assessed immediately thereafter for 30 s before return to the home cage. At 24 h following conditioning, mice were re-exposed to the experimental chamber for 3 min and freezing behavior was measured. Anymaze (Stoelting, Wood Dale, IL) software was used to analyze freezing behavior, which was defined as a lack of movement other than respiration [58].

Statistical analyses

Data were analyzed using either Student t-tests for two group comparisons or analysis of variance (ANOVA) techniques (SYSTAT 11.0 for Windows, SYSTAT Inc.) for multiple group comparisons followed by post hoc tests, using Bonferroni's or Tukey's correction, when necessary. For individual time points in LTP assessment, experimental groups were compared statistically by using the paired t-test for within-trial effects and the unpaired t-test for between-group effects. An alpha level of $p < 0.05$ was considered significant for all statistical tests used. Data are expressed as the mean ± standard error of the mean (SEM).

Results

Tat-induced astroglial pathology

To determine the extent to which Tat induction resulted in ultrastructural changes in astrocytes, electron microscopy of the hippocampal CA1 region was performed (Fig. 1). Criteria for identifying astrocytes and neurons are provided in the figure legends. While astroglia in Tat−/DOX mice appeared normal (Fig. 1*A*), pathologic changes were noted in many of the astrocytes in the CA1 region of Tat+/DOX mice (Fig. 1*B-F*). Unlike in Tat−/DOX-treated mice, the cytoplasm of astrocytes from Tat+/DOX animals showed a variety of different inclusions with features of lysosomes, autophagic vacuoles, and lamellar bodies (Fig. 1*B-E*). Importantly, the aberrant cytopathic features were not uniformly distributed within the astrocyte cytoplasm. Increased numbers of inclusions were typically present within distal cytoplasmic processes (Fig. 1*B,F*), and were only infrequently observed within the cell body adjacent to the nucleus (Fig. 1*C,D*). In addition, intranuclear vacuoles (Fig. 1*C,E*) as well as swollen rough endoplasmic reticulum (Fig. 1*B*) were also seen, although swollen rough endoplasmic reticulum was also occasionally seen in astroglia in Tat−/DOX mice.

Tat-induced reduction in dendritic spine density

To study the synaptic integrity of CA1 pyramidal neurons, Tat effects were assessed on apical dendritic spines, dendritic length, or morphology (Fig. 2*A*). Density of dendritic spines (spines/10 μm apical dendrite) in Golgi-Kopsch impregnated CA1 pyramidal neurons was significantly reduced in Tat+/DOX compared to Tat−/DOX mice ($p < 0.01$), but no effects were noted on dendritic length or dendritic morphology (Fig. 2*A*).

Neuron death was not evident following Tat induction

To assure that dendritic spine and synapse elimination was not accompanied by neuron death, the effect of Tat expression on DNA fragmentation in the hippocampal field CA1 was assessed (Fig. 2*B*). The proportion of $TUNEL^+$ neurons was unaffected by Tat induction and was less than 1% (Table 1). Our findings indicate that dendritic spine density was sensitive to Tat expression, but the reduction in spines was not accompanied by DNA fragmentation.

Tat-induced loss of synaptic integrity

To determine the nature and extent of the neuronal and synaptic response to Tat, CA1 pyramidal neurons were examined ultrastructurally (Fig. 2*C, D*). Unlike the more overt pathology in striatal medium spiny neurons seen in Golgi-silver preparations [51] and ultrastructurally [59], the dendrites of CA1 pyramidal neurons in Tat+/DOX mice only rarely showed degenerative changes. The dendrites of Tat+/DOX mice appeared to be relatively normal with no evidence of pathologic features such as neurofilament aggregates or dense inclusions.

Tat-induced significant changes in Syt2 and gephyrin

To determine the effects of Tat on specific synaptic proteins, we isolated protein lysates from the hippocampal CA1 region and evaluated synaptic proteins by immunoblot (Fig. 3*A,B*). Significant differences were only noted in two of the seven assessed synaptic proteins (Fig. 3*B*). The amount of Syt2 was significantly reduced in CA1 lysates of Tat+/DOX mice compared to controls ($p < 0.05$), whereas levels of gephyrin were significantly elevated in Tat+/DOX treated mice ($p < 0.05$). Syt2 and gephyrin are both associated with inhibitory synapses. To confirm and extend significant immunoblotting findings (Fig. 3C-F), immunofluorescence intensity within different layers of CA1 was compared across mouse strains. Findings revealed a significant decline in Syt2 immunofluorescence only within the

stratum radiatum in Tat+/DOX mice (Fig. 3C-D, $p < 0.01$). Alternatively, gephyrin immunofluorescence was more uniformly distributed within the CA1 region, and while its intensity appeared increased in all layers of CA1 of Tat+/DOX mice, these differences were not statistically significant (Fig. 3E-F).

Tat-induced disruption of LTP

To test whether the sublethal structural changes in hippocampal CA1 neurons interfere with synaptic function, field potentials were recorded in the stratum radiatum of area CA1 (Fig. 4*A*). The amplitudes of the field potentials were comparable in size in control and Tat+/DOX mice (Fig. 4*B*) and blocked by 20 μM DNQX (Fig. 4*C*), indicating that synaptic transmission was not compromised. To assess synaptic plasticity we examined LTP in hippocampal slices. Whereas, LTP was induced for Tat−/DOX mice (177.65 ± 1.91% of baseline) and was sustained for a 4 h duration, this did not occur for Tat+/DOX mice (92.89 ± 1.43% of baseline) (Fig. 4*D*). Hippocampal preparations from Tat+/DOX mice displayed transient potentiation during the initial peak response (137.48 ± 10.50% of baseline) but was not maintained and values fell back to baseline levels (91.42 ± 7.32%). Results demonstrate that LTP is dramatically inhibited or non-existent in hippocampal CA1 neurons following Tat induction.

Tat-induced disruption of spatial learning and memory

Since Tat induction disrupted synaptic function (LTP), we investigated effects of Tat expression on behavioral outcomes related to hippocampal function. Across the 5 acquisition training sessions, in the Morris water maze, ANOVA results revealed a Tat induction x session interaction for escape latency ($p < 0.05$, Fig. 5*A*) and travel distance ($p < 0.05$, Fig. 5*B*), indicating that with time, Tat−/DOX mice learned to find the hidden platform more rapidly than Tat+/DOX mice. Swim speed increased with time for both Tat−/DOX and Tat+/DOX mice ($p_{GG} < 0.001$, Fig. 5*C*), but no significant differences were noted between the 2 groups for any session. For the probe test, ANOVA results revealed a significant effect of Tat induction ($p < 0.05$), with Tat−/DOX animals swimming closer to the past target platform compared to Tat+/DOX mice (Fig. 5*D*), which was also observed when the time spent in each of the four quadrants was analyzed (Supplementary Results). Collectively, data indicate that disruption in synaptic function caused by Tat expression coincided with the onset and coordinated deterioration in spatial learning and memory.

Tat-induced disruption of memory in fear conditioning

Effects of Tat expression on memory were also noted in a fear-conditioning task. Tat+/DOX spent significantly less time freezing when re-exposed to a context associated with foot shock 24 h after conditioning than Tat−/DOX controls ($p < 0.01$, Fig. 6). There was no difference in freezing behavior among the groups either before or immediately after foot shock. Mice showed minimal freezing behavior 3 min before receiving the foot shock, while Tat−/DOX and Tat+/DOX animals exhibited a similar magnitude of freezing immediately after the shock. Despite the lack of initial differences, Tat+/DOX mice displayed significantly less freezing behavior after 24 h. This suggests that Tat expression results in memory consolidation and/or retrieval deficits.

Discussion

HAND persists even in cART-treated individuals who are aviremic [13-15, 60]. This suggests that once an individual becomes infected, restricting viral replication alone is insufficient to prevent neurocognitive damage. With improved survival in patients receiving cART, the manifestations of chronic exposure to low-levels of viral and cellular toxins associated with HIV-1 infection become increasingly evident – especially in sanctuaries

such as the brain with constrained immune surveillance and limited cART penetration [61]. Once CNS cells such as macrophages/microglia are infected, Tat production from pre-integration HIV-1 DNA or during the early phase of transcription from integrated proviral DNA is largely unaffected by current antiretroviral drugs [32]. For this reason, it is vital to determine the long-term effects of Tat on the CNS independent of the virus itself.

The Tat transgenic model is able to mimic HIV-1 as a chronic disease and has wide implications for understanding HAND. The non-lethal structural changes seen in the inducible Tat mice, with reductions in spine density and ultrastructural alterations in astrocytes, but without dendritic pathology and overt neuronal death, mirror the clinical features reported in patients with HAND [15]. Early in the hierarchy of HAND, including when asymptomatic neurocognitive impairment is evident, dendritic and synaptic damage without frank neuronal loss have been reported [9]. Although the root causes differ, synaptic damage *per se* is not unique to HIV-1, but underlies behavioral deficits in many other neurodegenerative disorders, such as Alzheimer's and Parkinson's diseases [62, 63]. There is prior evidence from different models that HIV-1, SIV, or Tat exposure can induce dendrite pathology [24, 46, 64-66], including damage to the molecular scaffolding of the postsynaptic element [67-69].

The significant decreases in Syt2 levels with *potential* corresponding increases in levels of gephyrin in Tat+/DOX mice suggest that Tat selectively targets inhibitory synapses associated with specific classes of hippocampal interneurons. Mismatched levels of Syt2 and gephyrin have similarly been reported in other murine models that exhibit hippocampal synaptic defects [56, 70]. While the reasons for the disparity are unclear, inhibitory postsynaptic neurons within the hippocampus have been proposed to compensate for defective or reduced quantities of nerve terminals by increasing the size of their postsynaptic apparati [56]. Moreover, similar compensatory mechanisms are well documented for other types of intercellular signaling in the CNS [e.g. 71]. Thus, the increases in gephyrin levels may represent an attempt to offset the reduction in $Syt2^+$ innervation [57] and the presumed decrease in inhibitory activity. A previous study in cerebral cortical neurons demonstrated that Tat30-86 increased presynaptic transmitter release, thereby increasing the frequency and amplitude of spontaneous miniature inhibitory postsynaptic currents (mIPSCs) in target neurons by 57% and 36%, respectively [72]. Because increased synaptic activity speeds the rate of postsynaptic density component turnover through enhanced degradation, and vice versa [73], decreased levels of inhibitory activity would be anticipated to augment gephyrin accumulation, which was observed in Tat+/DOX hippocampi. However, without measuring mIPSCs directly or establishing the time-course of Tat-induced changes, the mechanisms underlying dynamic changes in synaptic proteins in Tat+/DOX mice remain speculative. Lastly, the absence of changes in excitatory synaptic proteins were unexpected since Tat has been previously shown to decrease the number of $PSD\text{-}95^+$ synapses in hippocampal neurons by 50±7% through actions mediated via low-density lipoprotein receptor-related protein [50]. Although our findings indicate that Tat preferentially interferes with inhibitory synapses in CA1, additional studies are needed to elucidate the mechanisms involved and whether the loss of $Syt2^+$ afferents to the stratum radiatum of CA1 might be preceded by excitotoxic injury to subsets of inhibitory neurons following Tat exposure.

Tat-induced synaptodendritic alterations in the hippocampus coincide with disruptions in synaptic function (LTP) in CA1 pyramidal neurons and with defects in learning and memory examined in this study. The dramatic effects of Tat induction on neuronal function suggest the profound importance of this protein in the pathogenesis of HAND. Similar deleterious effects of alcohol on memory are well known and have been shown to occur via inhibition of NMDA receptor-dependent LTP in the hippocampus [74]. Because there is only a subtle ~10% reduction in spine density, and no change in dendrite length, dendritic pathology, or

the synaptic vesicle-associated proteins Syn, Gad67, VGluT2, VGluT1, and PSD-95, it is not surprising that basal synaptic transmission is not altered. A variety of mouse models report normal basal synaptic transmission, despite significant alterations in LTP [75-77].

Findings of Tat-induced functional and behavioral deficits have been reported previously [72, 78-80]. However, in contrast to our chronic disease model, previous studies have looked at more acute Tat exposure *in vitro* and/or *in vivo*. Li and colleagues [79] examined the effects of a single intracerebroventricular injection of Tat. This study has some methodological limitations, including (i) the use of a single exposure to an artificially high concentration of Tat, and (ii) the potential exacerbation of Tat effects by the primary injury itself or *vice versa* [79]. We speculate that the pathophysiologic signals underlying the loss of synapses with sustained exposure to "physiologic" levels of Tat in HIV-1 infection differs markedly from pro-apoptotic signals caused by acute exposure to high concentrations of Tat.

An unanswered question is to what extent the reported modest structural changes in this study lead to the neurocognitive impairments seen in Tat transgenic mice and whether these changes are reversible. A recent study using a transgenic mouse model of Alzheimer's disease has shown that sustained deficits in dendritic structure and function are reversible [81]. In our model, the Tat-induced cumulative reductions in synaptic organization and function occur in the absence of neuronal death. We assume that NMDARs at both "synaptic" and "extrasynaptic" sites and/or specific subunit configurations, such as NR2B, which are targeted by the Tat protein [19, 39, 82] and contribute to excitotoxic neuronal damage [83, 84], are operative in our model. Our findings additionally suggest that Syt2-expressing GABAergic presynaptic terminals are vulnerable to Tat. Indeed, reductions in inhibitory $Syt2^+$ synapses may lower the threshold for excitation contributing to neuronal dysfunction and the probability of excitotoxic injury. From this perspective, and contrary to our earlier conclusion, it could be speculated that increases in gephyrin, which organizes specific $GABA_A$-receptor subtypes at inhibitory postsynaptic sites [85, 86], may be an adaptive response to excessive glutamatergic signals. Although we did not see changes in the levels of excitatory synaptic proteins, we did see subtle reductions in dendritic spines and cannot exclude the possibility that this represents the initial stages of excitatory synaptic remodeling [87, 88]. Assuming the initial molecular changes at the synapse can be prevented or reversed, then agents that counter the effects of Tat, if given early during HAND, may potentially reverse the synaptodendritic dystrophy and rescue degenerating neurons, resulting in improved cognition and behavior.

Within the CNS, the striatum and hippocampus are especially vulnerable to HIV-1 infection [64, 89-91]. Parkinsonian features are reported in some HIV-1-infected patients, suggesting striatal dysfunction [92], while some of the highest proviral DNA levels are reported in the hippocampus [93]. A prior study in striatal spiny neurons demonstrated that expression of the Tat transgene reduced spine density, while causing dendritic varicosities and fragmentation without corresponding neuron losses [51]. Accordingly, the present hippocampal findings should be interpreted cautiously with the understanding that Tat impacts other brain regions. Changes in complex behavioral and cognitive outcomes likely reflect the collective effects of multiple Tat insults in interrelated brain areas. Interestingly, one parameter appears to be more adversely affected by Tat expression in the striatum than in the hippocampus [51]. As reported in the present study, dendritic degeneration (varicosities and fragmentation) was not seen in the hippocampus, in contrast to previous reports in the striatum [51]. Notably, however, the deficits observed in the Morris water maze and fear-conditioning paradigm can be attributed to disruption of learning and memory, which also has been reported in an alternative Tat transgenic mouse [80]. No effects on sensorimotor function were noted as travel speed in the Morris water maze task and baseline freezing behavior in the fear-conditioning task were not different between Tat

−/DOX and Tat+/DOX mice. The findings on dendritic degeneration mentioned above argue for regional differences in the susceptibility of neurons to Tat, which have also been described in glia [94]. Heterogeneity of viral load in different brain regions has also been documented in brain tissues of HIV-1-infected patients in [95].

Collectively, the inducible Tat transgenic mouse appears to be a highly relevant model for examining the protracted loss of connectivity and sublethal dendrite degeneration in HIV-1 that occurs in the absence of, or long before, the advent of frank neuronal apoptosis. The findings in the present study demonstrate that Tat exposure results in profound functional changes in synaptic physiology (loss of LTP) and in behavior. Despite pronounced functional losses, the structural abnormalities were more modest. A selective reduction in the density of inhibitory Syt2-containing nerve terminals was accompanied by subtle increases in gephyrin expression and a decreased density of apical dendritic spines in CA1 pyramidal neurons. We propose that while Tat expression does cause key functional and behavioral deficits, which underlie key features of HAND, these are likely to be occurring at the molecular level and influencing synaptic function and organization.

Supplementary Material

Refer to Web version on PubMed Central for supplementary material.

Acknowledgments

We gratefully acknowledge the support from the National Eye Institute (R01 EY012716) and the National Institute on Drug Abuse (NIDA R01 DA018633, P01 DA019398, and K02 DA027374). Further, microscopy was performed at the VCU Department of Anatomy and Neurobiology Microscopy Facility, supported, in part, with funding from NIH-NINDS Center core grant (P30 NS047463).

References

1. Hebb, DO. The organization of behavior. Wiley & Sons; New York: 1949.
2. Dayhoff JE. Computational properties of networks of synchronous groups of spiking neurons. Neural Comput. 2007; 19:2433–2467. [PubMed: 17650065]
3. Globus A, Scheibel AB. Loss of dendrite spines as an index of pre-synaptic terminal patterns. Nature. 1966; 212:463–465. [PubMed: 5339139]
4. Kruman I, Nath A, Mattson MP. HIV-1 protein Tat induces apoptosis of hippocampal neurons by a mechanism involving caspase activation, calcium overload, and oxidative stress. Exp Neurol. 1998; 154:276–288. [PubMed: 9878167]
5. Sheng M, Kim MJ. Postsynaptic signaling and plasticity mechanisms. Science. 2002; 298:776–780. [PubMed: 12399578]
6. Tada T, Sheng M. Molecular mechanisms of dendritic spine morphogenesis. Curr Opin Neurobiol. 2006; 16:95–101. [PubMed: 16361095]
7. Mattson MP, Gleichmann M, Cheng A. Mitochondria in neuroplasticity and neurological disorders. Neuron. 2008; 60:748–766. [PubMed: 19081372]
8. Masliah E, Heaton RK, Marcotte TD, Ellis RJ, Wiley CA, Mallory M, et al. Dendritic injury is a pathological substrate for human immunodeficiency virus-related cognitive disorders. HNRC Group. The HIV Neurobehavioral Research Center. Ann Neurol. 1997; 42:963–972. [PubMed: 9403489]
9. Everall IP, Heaton RK, Marcotte TD, Ellis RJ, McCutchan JA, Atkinson JH, et al. Cortical synaptic density is reduced in mild to moderate human immunodeficiency virus neurocognitive disorder. HNRC Group. HIV Neurobehavioral Research Center. Brain Pathol. 1999; 9:209–217. [PubMed: 10219738]
10. Scheibel AB. The hippocampus: organizational patterns in health and senescence. Mech Ageing Dev. 1979; 9:89–102. [PubMed: 439952]

11. Day M, Wang Z, Ding J, An X, Ingham CA, Shering AF, et al. Selective elimination of glutamatergic synapses on striatopallidal neurons in Parkinson disease models. Nat Neurosci. 2006; 9:251–259. [PubMed: 16415865]
12. Ellis R, Langford D, Masliah E. HIV and antiretroviral therapy in the brain: neuronal injury and repair. Nat Rev Neurosci. 2007; 8:33–44. [PubMed: 17180161]
13. Heaton RK, Clifford DB, Franklin DR Jr. Woods SP, Ake C, Vaida F, et al. HIV-associated neurocognitive disorders persist in the era of potent antiretroviral therapy: CHARTER Study. Neurology. 2010; 75:2087–2096. [PubMed: 21135382]
14. Heaton RK, Franklin DR, Ellis RJ, McCutchan JA, Letendre SL, Leblanc S, et al. HIV-associated neurocognitive disorders before and during the era of combination antiretroviral therapy: differences in rates, nature, and predictors. J Neurovirol. 2010
15. McArthur JC, Steiner J, Sacktor N, Nath A. Human immunodeficiency virus-associated neurocognitive disorders: mind the gap. Ann Neurol. 2010; 67:699–714. [PubMed: 20517932]
16. Coleman P, Federoff H, Kurlan R. A focus on the synapse for neuroprotection in Alzheimer disease and other dementias. Neurology. 2004; 63:1155–1162. [PubMed: 15477531]
17. Brenneman DE, Westbrook GL, Fitzgerald SP, Ennist DL, Elkins KL, Ruff MR, et al. Neuronal cell killing by the envelope protein of HIV and its prevention by vasoactive intestinal peptide. Nature. 1988; 335:639–642. [PubMed: 2845276]
18. Lipton SA. Human immunodeficiency virus-infected macrophages, gp120, and N-methyl-D-aspartate receptor-mediated neurotoxicity. Ann Neurol. 1993; 33:227–228. [PubMed: 8434889]
19. Haughey NJ, Holden CP, Nath A, Geiger JD. Involvement of inositol 1,4,5-trisphosphate-regulated stores of intracellular calcium in calcium dysregulation and neuron cell death caused by HIV-1 protein Tat. J Neurochem. 1999; 73:1363–1374. [PubMed: 10501179]
20. Nath A. Human immunodeficiency virus (HIV) proteins in neuropathogenesis of HIV dementia. J Infect Dis. 2002; 186(Suppl 2):S193–198. [PubMed: 12424697]
21. Jones GJ, Barsby NL, Cohen EA, Holden J, Harris K, Dickie P, et al. HIV-1 Vpr causes neuronal apoptosis and in vivo neurodegeneration. J Neurosci. 2007; 27:3703–3711. [PubMed: 17409234]
22. Dreyer EB, Kaiser PK, Offermann JT, Lipton SA. HIV-1 coat protein neurotoxicity prevented by calcium channel antagonists. Science. 1990; 248:364–367. [PubMed: 2326646]
23. Lipton SA. HIV-related neurotoxicity. Brain Pathol. 1991; 1:193–199. [PubMed: 1669708]
24. Kaul M, Garden GA, Lipton SA. Pathways to neuronal injury and apoptosis in HIV-associated dementia. Nature. 2001; 410:988–994. [PubMed: 11309629]
25. Sodroski J, Patarca R, Rosen C, Wong-Staal F, Haseltine W. Location of the trans-activating region on the genome of human T-cell lymphotropic virus type III. Science. 1985; 229:74–77. [PubMed: 2990041]
26. Ensoli B, Buonaguro L, Barillari G, Fiorelli V, Gendelman R, Morgan RA, et al. Release, uptake, and effects of extracellular human immunodeficiency virus type 1 Tat protein on cell growth and viral transactivation. J Virol. 1993; 67:277–287. [PubMed: 8416373]
27. Chang HC, Samaniego F, Nair BC, Buonaguro L, Ensoli B. HIV-1 Tat protein exits from cells via a leaderless secretory pathway and binds to extracellular matrix-associated heparan sulfate proteoglycans through its basic region. AIDS. 1997; 11:1421–1431. [PubMed: 9342064]
28. Karn J. Tackling Tat. J Mol Biol. 1999; 293:235–254. [PubMed: 10550206]
29. Lin X, Irwin D, Kanazawa S, Huang L, Romeo J, Yen TS, et al. Transcriptional profiles of latent human immunodeficiency virus in infected individuals: effects of Tat on the host and reservoir. J Virol. 2003; 77:8227–8236. [PubMed: 12857891]
30. Richter SN, Palu G. Inhibitors of HIV-1 Tat-mediated transactivation. Curr Med Chem. 2006; 13:1305–1315. [PubMed: 16712471]
31. Ensoli B, Fiorelli V, Ensoli F, Cafaro A, Titti F, Butto S, et al. Candidate HIV-1 Tat vaccine development: from basic science to clinical trials. AIDS. 2006; 20:2245–2261. [PubMed: 17117011]
32. Wu Y. HIV-1 gene expression: lessons from provirus and non-integrated DNA. Retrovirology. 2004; 1:13. [PubMed: 15219234]

33. Bonavia R, Bajetto A, Barbero S, Albini A, Noonan DM, Schettini G. HIV-1 Tat causes apoptotic death and calcium homeostasis alterations in rat neurons. Biochem Biophys Res Commun. 2001; 288:301–308. [PubMed: 11606043]
34. Haughey NJ, Nath A, Mattson MP, Slevin JT, Geiger JD. HIV-1 Tat through phosphorylation of NMDA receptors potentiates glutamate excitotoxicity. J Neurochem. 2001; 78:457–467. [PubMed: 11483648]
35. Lai Y, Du L, Dunsmore KE, Jenkins LW, Wong HR, Clark RS. Selectively increasing inducible heat shock protein 70 via TAT-protein transduction protects neurons from nitrosative stress and excitotoxicity. J Neurochem. 2005; 94:360–366. [PubMed: 15998287]
36. Mattson MP, Haughey NJ, Nath A. Cell death in HIV dementia. Cell Death Differ. 2005; 12(Suppl 1):893–904. [PubMed: 15761472]
37. King JE, Eugenin EA, Buckner CM, Berman JW. HIV Tat and neurotoxicity. Microbes Infect. 2006; 8:1347–1357. [PubMed: 16697675]
38. Eugenin EA, King JE, Nath A, Calderon TM, Zukin RS, Bennett MV, et al. HIV-Tat induces formation of an LRP-PSD-95-NMDAR-nNOS complex that promotes apoptosis in neurons and astrocytes. Proc Natl Acad Sci U S A. 2007; 104:3438–3443. [PubMed: 17360663]
39. Li W, Huang Y, Reid R, Steiner J, Malpica-Llanos T, Darden TA, et al. NMDA receptor activation by HIV-Tat protein is clade dependent. J Neurosci. 2008; 28:12190–12198. [PubMed: 19020013]
40. Eugenin EA, King JE, Hazleton JE, Major EO, Bennett MV, Zukin RS, et al. Differences in NMDA receptor expression during human development determine the response of neurons to HIV-Tat-mediated neurotoxicity. Neurotox Res. 2010; 19:138–148. [PubMed: 20094923]
41. Self RL, Mulholland PJ, Nath A, Harris BR, Prendergast MA. The human immunodeficiency virus type-1 transcription factor Tat produces elevations in intracellular Ca^{2+} that require function of an N-methyl-D-aspartate receptor polyamine-sensitive site. Brain Res. 2004; 995:39–45. [PubMed: 14644469]
42. Singh IN, Goody RJ, Dean C, Ahmad NM, Lutz SE, Knapp PE, et al. Apoptotic death of striatal neurons induced by human immunodeficiency virus-1 Tat and gp120: Differential involvement of caspase-3 and endonuclease G. J Neurovirol. 2004; 10:141–151. [PubMed: 15204919]
43. Ensoli B, Bellino S, Tripiciano A, Longo O, Francavilla V, Marcotullio S, et al. Therapeutic immunization with HIV-1 Tat reduces immune activation and loss of regulatory T-cells and improves immune function in subjects on HAART. PLoS One. 2010; 5:e13540. [PubMed: 21085635]
44. Bruce-Keller AJ, Turchan-Cholewo J, Smart EJ, Geurin T, Chauhan A, Reid R, et al. Morphine causes rapid increases in glial activation and neuronal injury in the striatum of inducible HIV-1 Tat transgenic mice. Glia. 2008; 56:1414–1427. [PubMed: 18551626]
45. Mattson MP, Keller JN, Begley JG. Evidence for synaptic apoptosis. Exp Neurol. 1998; 153:35–48. [PubMed: 9743565]
46. Sa MJ, Madeira MD, Ruela C, Volk B, Mota-Miranda A, Paula-Barbosa MM. Dendritic changes in the hippocampal formation of AIDS patients: a quantitative Golgi study. Acta Neuropathol. 2004; 107:97–110. [PubMed: 14605830]
47. Bellizzi MJ, Lu SM, Masliah E, Gelbard HA. Synaptic activity becomes excitotoxic in neurons exposed to elevated levels of platelet-activating factor. J Clin Invest. 2005; 115:3185–3192. [PubMed: 16276420]
48. Perry SW, Norman JP, Litzburg A, Zhang D, Dewhurst S, Gelbard HA. HIV-1 transactivator of transcription protein induces mitochondrial hyperpolarization and synaptic stress leading to apoptosis. J Immunol. 2005; 174:4333–4344. [PubMed: 15778398]
49. Philippon V, Vellutini C, Gambarelli D, Harkiss G, Arbuthnott G, Metzger D, et al. The basic domain of the lentiviral Tat protein is responsible for damages in mouse brain: involvement of cytokines. Virology. 1994; 205:519–529. [PubMed: 7526541]
50. Kim HJ, Martemyanov KA, Thayer SA. Human immunodeficiency virus protein Tat induces synapse loss via a reversible process that is distinct from cell death. J Neurosci. 2008; 28:12604–12613. [PubMed: 19036954]

51. Fitting S, Xu R, Bull C, Buch SK, El-Hage N, Nath A, et al. Interactive comorbidity between opioid drug abuse and HIV-1 Tat: chronic exposure augments spine loss and sublethal dendritic pathology in striatal neurons. Am J Pathol. 2010; 177:1397–1410. [PubMed: 20651230]
52. Hauser KF, McLaughlin PJ, Zagon IS. Endogenous opioid systems and the regulation of dendritic growth and spine formation. J Comp Neurol. 1989; 281:13–22. [PubMed: 2925898]
53. Hauser KF, Hahn YK, Adjan VV, Zou S, Buch SK, Nath A, et al. HIV-1 Tat and morphine have interactive effects on oligodendrocyte survival and morphology. Glia. 2009; 57:194–206. [PubMed: 18756534]
54. Fox MA, Sanes JR. Synaptotagmin I and II are present in distinct subsets of central synapses. J Comp Neurol. 2007; 503:280–296. [PubMed: 17492637]
55. Fox MA, Sanes JR, Borza DB, Eswarakumar VP, Fassler R, Hudson BG, et al. Distinct target-derived signals organize formation, maturation, and maintenance of motor nerve terminals. Cell. 2007; 129:179–193. [PubMed: 17418794]
56. Su J, Gorse K, Ramirez F, Fox MA. Collagen XIX is expressed by interneurons and contributes to the formation of hippocampal synapses. J Comp Neurol. 2010; 518:229–253. [PubMed: 19937713]
57. Henny P, Jones BE. Innervation of orexin/hypocretin neurons by GABAergic, glutamatergic or cholinergic basal forebrain terminals evidenced by immunostaining for presynaptic vesicular transporter and postsynaptic scaffolding proteins. J Comp Neurol. 2006; 499:645–661. [PubMed: 17029265]
58. Blanchard RJ, Blanchard DC. Crouching as an index of fear. J Comp Physiol Psychol. 1969; 67:370–375. [PubMed: 5787388]
59. Hauser KF, Fitting S, Dever SM, Podhaizer EM, Knapp PE. Opiate drug use and the pathophysiology of NeuroAIDS. Current HIV Research. May 11.2012 [Epub ahead of print].
60. Clifford DB. HIV-associated neurocognitive disease continues in the antiretroviral era. Top HIV Med. 2008; 16:94–98. [PubMed: 18591717]
61. Schouten J, Cinque P, Gisslen M, Reiss P, Portegies P. HIV-1 infection and cognitive impairment in the cART era: a review. AIDS. 2011; 25:561–575. [PubMed: 21160410]
62. Reddy PH, Beal MF. Amyloid beta, mitochondrial dysfunction and synaptic damage: implications for cognitive decline in aging and Alzheimer's disease. Trends Mol Med. 2008; 14:45–53. [PubMed: 18218341]
63. van Spronsen M, Hoogenraad CC. Synapse pathology in psychiatric and neurologic disease. Curr Neurol Neurosci Rep. 2010; 10:207–214. [PubMed: 20425036]
64. Masliah E, Ge N, Achim CL, Hansen LA, Wiley CA. Selective neuronal vulnerability in HIV encephalitis. J Neuropathol Exp Neurol. 1992; 51:585–593. [PubMed: 1484289]
65. Nath A, Geiger J. Neurobiological aspects of human immunodeficiency virus infection: neurotoxic mechanisms. Prog Neurobiol. 1998; 54:19–33. [PubMed: 9460791]
66. Gonzalez-Scarano F, Martin-Garcia J. The neuropathogenesis of AIDS. Nat Rev Immunol. 2005; 5:69–81. [PubMed: 15630430]
67. Zheng J, Zhuang W, Yan N, Kou G, Peng H, McNally C, et al. Classification of HIV-1-mediated neuronal dendritic and synaptic damage using multiple criteria linear programming. Neuroinformatics. 2004; 2:303–326. [PubMed: 15365193]
68. Cheng A, Hou Y, Mattson MP. Mitochondria and neuroplasticity. ASN Neuro. 2010; 2:e00045. [PubMed: 20957078]
69. Bingol B, Sheng M. Deconstruction for reconstruction: the role of proteolysis in neural plasticity and disease. Neuron. 2011; 69:22–32. [PubMed: 21220096]
70. Rodenas-Ruano A, Perez-Pinzon MA, Green EJ, Henkemeyer M, Liebl DJ. Distinct roles for ephrinB3 in the formation and function of hippocampal synapses. Dev Biol. 2006; 292:34–45. [PubMed: 16466709]
71. Rice DS, Sheldon M, D'Arcangelo G, Nakajima K, Goldowitz D, Curran T. Disabled-1 acts downstream of Reelin in a signaling pathway that controls laminar organization in the mammalian brain. Development. 1998; 125:3719–3729. [PubMed: 9716537]

72. Brailoiu GC, Brailoiu E, Chang JK, Dun NJ. Excitatory effects of human immunodeficiency virus 1 Tat on cultured rat cerebral cortical neurons. Neuroscience. 2008; 151:701–710. [PubMed: 18164555]
73. Ehlers MD. Activity level controls postsynaptic composition and signaling via the ubiquitin-proteasome system. Nat Neurosci. 2003; 6:231–242. [PubMed: 12577062]
74. Hicklin TR, Wu PH, Radcliffe RA, Freund RK, Goebel-Goody SM, Correa PR, et al. Alcohol inhibition of the NMDA receptor function, long-term potentiation, and fear learning requires striatal-enriched protein tyrosine phosphatase. Proc Natl Acad Sci U S A. 2011; 108:6650–6655. [PubMed: 21464302]
75. Shum FW, Wu LJ, Zhao MG, Toyoda H, Xu H, Ren M, et al. Alteration of cingulate long-term plasticity and behavioral sensitization to inflammation by environmental enrichment. Learn Mem. 2007; 14:304–312. [PubMed: 17522019]
76. Soderling TR, Derkach VA. Postsynaptic protein phosphorylation and LTP. Trends Neurosci. 2000; 23:75–80. [PubMed: 10652548]
77. Petrone A, Battaglia F, Wang C, Dusa A, Su J, Zagzag D, et al. Receptor protein tyrosine phosphatase alpha is essential for hippocampal neuronal migration and long-term potentiation. EMBO J. 2003; 22:4121–4131. [PubMed: 12912911]
78. Behnisch T, Francesconi W, Sanna PP. HIV secreted protein Tat prevents long-term potentiation in the hippocampal CA1 region. Brain Res. 2004; 1012:187–189. [PubMed: 15158177]
79. Li ST, Matsushita M, Moriwaki A, Saheki Y, Lu YF, Tomizawa K, et al. HIV-1 Tat inhibits long-term potentiation and attenuates spatial learning [corrected]. Ann Neurol. 2004; 55:362–371. [PubMed: 14991814]
80. Carey AN, Sypek EI, Singh HD, Kaufman MJ, McLaughlin JP. Expression of HIV-Tat protein is associated with learning and memory deficits in the mouse. Behav Brain Res. 2011; 229:48–56. [PubMed: 22197678]
81. Smith DL, Pozueta J, Gong B, Arancio O, Shelanski M. Reversal of long-term dendritic spine alterations in Alzheimer disease models. Proc Natl Acad Sci U S A. 2009; 106:16877–16882. [PubMed: 19805389]
82. Strijbos PJ, Zamani MR, Rothwell NJ, Arbuthnott G, Harkiss G. Neurotoxic mechanisms of transactivating protein Tat of Maedi-Visna virus. Neurosci Lett. 1995; 197:215–218. [PubMed: 8552302]
83. Liu Y, Wong TP, Aarts M, Rooyakkers A, Liu L, Lai TW, et al. NMDA receptor subunits have differential roles in mediating excitotoxic neuronal death both in vitro and in vivo. J Neurosci. 2007; 27:2846–2857. [PubMed: 17360906]
84. Soriano FX, Hardingham GE. Compartmentalized NMDA receptor signalling to survival and death. J Physiol. 2007; 584:381–387. [PubMed: 17690142]
85. Fritschy JM, Harvey RJ, Schwarz G. Gephyrin: where do we stand, where do we go? Trends Neurosci. 2008; 31:257–264. [PubMed: 18403029]
86. Luscher B, Keller CA. Regulation of GABAA receptor trafficking, channel activity, and functional plasticity of inhibitory synapses. Pharmacol Ther. 2004; 102:195–221. [PubMed: 15246246]
87. Kim MJ, Futai K, Jo J, Hayashi Y, Cho K, Sheng M. Synaptic accumulation of PSD-95 and synaptic function regulated by phosphorylation of serine-295 of PSD-95. Neuron. 2007; 56:488–502. [PubMed: 17988632]
88. Bourne JN, Harris KM. Balancing structure and function at hippocampal dendritic spines. Annu Rev Neurosci. 2008; 31:47–67. [PubMed: 18284372]
89. Fujimura RK, Goodkin K, Petito CK, Douyon R, Feaster DJ, Concha M, et al. HIV-1 proviral DNA load across neuroanatomic regions of individuals with evidence for HIV-1-associated dementia. J Acquir Immune Defic Syndr Hum Retrovirol. 1997; 16:146–152. [PubMed: 9390565]
90. Wiley CA, Soontornniyomkij V, Radhakrishnan L, Masliah E, Mellors J, Hermann SA, et al. Distribution of brain HIV load in AIDS. Brain Pathol. 1998; 8:277–284. [PubMed: 9546286]
91. Moore DJ, Masliah E, Rippeth JD, Gonzalez R, Carey CL, Cherner M, et al. Cortical and subcortical neurodegeneration is associated with HIV neurocognitive impairment. AIDS. 2006; 20:879–887. [PubMed: 16549972]

92. Koutsilieri E, Sopper S, Scheller C, ter Meulen V, Riederer P. Parkinsonism in HIV dementia. J Neural Transm. 2002; 109:767–775. [PubMed: 12111466]

93. Fujimura RK, Bockstahler LE. Polymerase chain reaction method for determining ratios of human immunodeficiency virus proviral DNA to cellular genomic DNA in brain tissues of HIV-infected patients. J Virol Methods. 1995; 55:309–325. [PubMed: 8609197]

94. Fitting S, Zou S, Chen W, Vo P, Hauser KF, Knapp PE. Regional heterogeneity and diversity in cytokine and chemokine production by astroglia: differential responses to HIV-1 Tat, gp120, and morphine revealed by multiplex analysis. J Proteome Res. 2010; 9:1795–1804. [PubMed: 20121167]

95. Sei S, Saito K, Stewart SK, Crowley JS, Brouwers P, Kleiner DE, et al. Increased human immunodeficiency virus (HIV) type 1 DNA content and quinolinic acid concentration in brain tissues from patients with HIV encephalopathy. J Infect Dis. 1995; 172:638–647. [PubMed: 7658054]

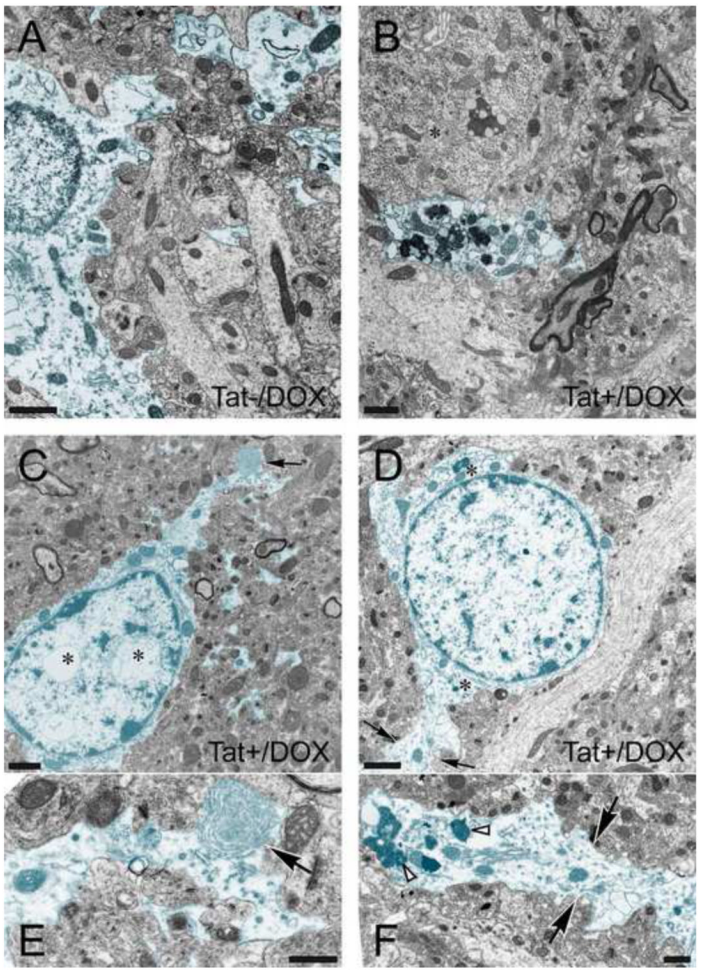

Figure 1.

Effects of Tat induction on the ultrastructure of astrocytes in CA1 region of the hippocampus (2-3-mo old mice). Astrocytes (highlighted in blue) from (A) control (Tat−/DOX) and (B-F) inducible, doxycycline (DOX) exposed Tat transgenic (Tat+/DOX) mice. (A) Astroglia in Tat−/DOX mice appear normal, displaying little or no pathology compared to astrocytes from Tat+/DOX animals. Grey matter astrocytes are distinguished from neurons by their lighter cytoplasm, are bordered by an irregular plasma membranes, lack organized cisternae of rough and large numbers of free ribosomes, lack microtubule bundles, possess more watery cytoplasm, and lack of synaptic contacts. (B-F) Astroglia in Tat+/DOX mice display increased numbers of inclusions with the features of lysosomes, autophagic vacuoles, and lamellar bodies compared to Tat−/DOX mice. In addition, the perikaryon above the astrocytic processes is that of a neuron (B, *). Note the abundance of endoplasmic reticulum-associated ribosomal clusters (Nissl bodies) and higher density of free ribosomes in the cytoplasm. (C) Whorls of membrane were occasionally seen within distal astrocyte processes (black arrow) shown at higher magnification in (E). Intranuclear vacuoles were present within the astrocyte cell body (D, *). (D) In the astrocyte highlighted in blue note the paucity of free ribosomes in the cytoplasm and very sparse rough endoplasmic reticulum (*). The black arrows denote the distal process of this astrocyte shown at higher magnification in (F). Numerous electron dense inclusions (white arrowheads) and vacuoles are present in this process. Scale bar for (A-D) = 1 μm, Scale bar for (E-F) = 0.5 μm.

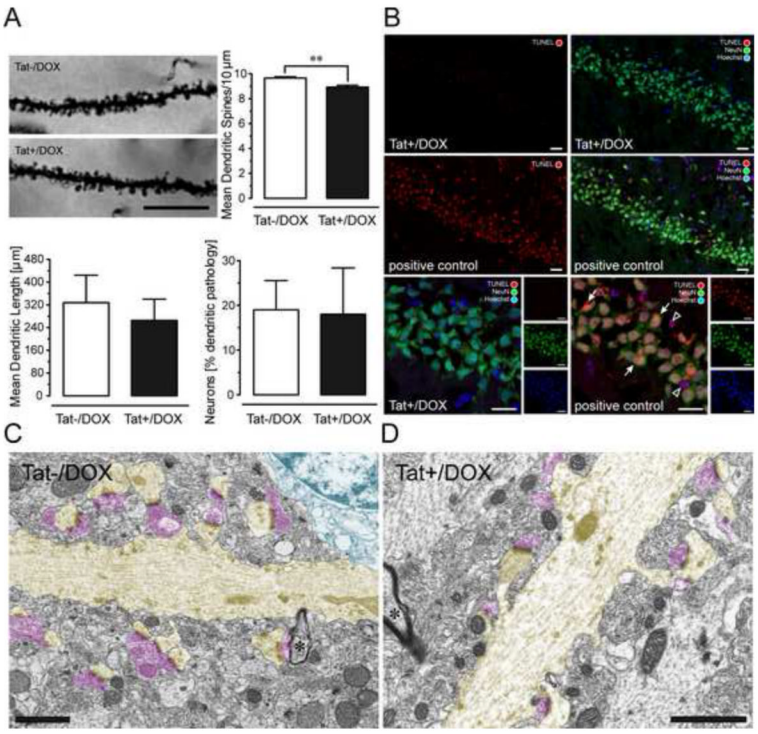

Figure 2.

(A) Effects of Tat induction on number of dendritic spines, dendritic length, and morphology on pyramidal neurons in the stratum radiatum of the hippocampal field CA1 (2-3-mo old mice). Spine density was assessed in Golgi-Kopsch impregnated neurons. Scale bars = 10 μm. Number of dendritic spines were counted on apical dendrites, recorded as the mean number of spines per 10 μm dendrite length, averaged for each animal, and reported as changes in the mean spine density (number of spines/10 μm). Significant decreases in total spine density were seen in the inducible (Tat+/DOX, $n = 6$) mice following induction with DOX compared to control (Tat−/DOX, $n = 6$) mice [$^{**}t(10) = 3.89$, $p < 0.01$]. Length of apical dendrites was measured, since afferent synapses arriving from the Schaffer collaterals (see LTP studies below) preferentially ramify on apical dendrites within the stratum radiatum. For morphological assessment, each neuron was categorized either as having apical dendrites with an entirely normal morphology, or having an abnormal morphology, with one or more dendrites that displayed aberrant features, such as beading and fragmentation along proximal and/or distal segments [see also 51]. The proportion of neurons that possessed one or more dendrites with abnormal morphology was counted and reported as a percentage of total neurons examined. No effects were noted on dendritic length or dendritic morphology. Data are represented as mean (± SEM). (B) Effects of Tat induction on TUNEL detection in NeuN immunoreactive pyramidal neurons in the hippocampal field CA1. TUNEL was employed to detect in situ DNA fragmentation using the In Situ Cell Death Detection Kit, TMR red (Roche Applied Science, Indianapolis, IN). Positive control tissue for the TUNEL reaction was incubated with micrococcal nuclease or recombinant DNase I for 10 min at +15 to 25°C to induce DNA strand breaks prior to the TUNEL labeling procedure. TUNEL detection was almost never detected in the Tat+/DOX group ($n = 4$), whereas most Neu-N(+) and NeuN(−) TUNEL-positive cells were abundant in the positive control. The positive control indicates DNA fragmentation for NeuN immunoreactive neurons in the CA1 layer (arrow) as well as in cells that were not NeuN immunostained, likely representing glia (open arrowhead); DOX: doxycycline. (C-D)

Electron micrographs of dendrites and associated postsynaptic spines (highlighted in yellow) in the CA1 region of the hippocampus of Tat+/DOX mice. Dendrites are distinguished from myelinated axons by their lighter cytoplasm, abundant microtubules, thicker diameter, and dendritic spines. The asterisk indicates a myelinated axon (*). Note continuity of dendrites with their spinous processes. Despite loss of function shown in Fig. 4 and changes in synaptic proteins shown in Fig. 3, the ultrastructure looks relatively normal in Tat+/DOX mice (D) comparable to Tat−/DOX mice (C). Both asymmetric synapses contacting dendritic spines, as well as the symmetric synapses on the dendritic shaft appeared qualitatively normal. Pre-synaptic elements highlighted in pink; Scale bar = 1 μm.

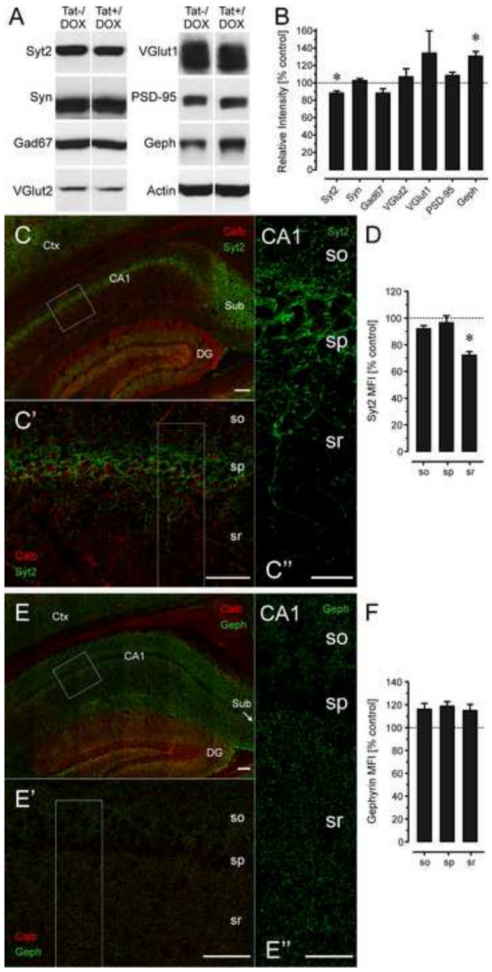

Figure 3.

Effects of Tat induction on levels of synaptic markers by immunoblotting (A-B) and immunohistochemistry (C-F) in the CA1 region of the hippocampus of 3-mo old Tat−/DOX ($n = 3$) and Tat+/DOX ($n = 3$) mice. (A-B) Immunoblots demonstrate significant reductions in Syt2 [$t(4) = 2.58$, $p < 0.05$] and significant increases in gephyrin [$t(4) = 2.24$, $p < 0.05$] levels in Tat+/DOX compared to Tat−/DOX lysates, while levels of Syn, VGlut1, VGlut12, or PSD-95 were not markedly affected when normalized to actin levels. Significant decreases in Syt2 levels with corresponding increases in levels of gephyrin in Tat+/DOX mice suggest that Tat selectively targets inhibitory synapses associated with specific classes of hippocampal interneurons. (C-F) Syt2 (fixed tissue, green, C-D) or gephyrin (fresh tissue, green, E-F) MFI was determined from optical sections double-labeled with calbindin (red). (C-C'') $Syt2^+$ nerve terminals (green) are specifically present in the stratum pyramidalis of the CA1 region and sparsely distributed throughout the stratum oriens and stratum radiatum. C' and C'' are higher magnification images shown in rectangles in C and C', respectively. (D) The density of $Syt2^+$ nerve terminals was dramatically and selectively decreased for Tat +/DOX mice in the stratum radiatum of CA1 compared to the Tat−/DOX mice [$t(4) = 4.00$, $p < 0.01$], while corresponding reductions in $Syt2^+$ terminals were not evident in the stratum pyramidal or stratum oriens. (E-E'') $Gephyrin^+$ postsynaptic puncta (green) were uniformly distributed throughout the stratum oriens and stratum radiatum, but displaying reduced density in the stratum pyramidalis that coincided with the physical presence of the pyramidal neuron perikarya. E' and E'' are higher magnification images shown in rectangles in E and

E', respectively. Although gephyrin MFI shows a decline in the stratum pyramidalis, this was consistent in Tat−/DOX and Tat+/DOX mice such that no relative difference was noted when comparing the two strains (F). Dashed lines represent control levels. Data are mean ± SEM. *$p < 0.05$; Syt2: synaptotagmin 2; Syn: Synapsin; Gad67: glutamate decarboxylase 67; VGlut1: vesicular glutamate transporters 1; VGlut2: vesicular glutamate transporters 2; PSD-95: postsynaptic density protein 95; Geph: gephyrin; Scale bars = 100 μ*m in C and E (20x objective), 50* μ*m in C' and E' (63x objective), 20* μm in C'' and E'' (63x objective); CA1: Cornu ammonis 1 region; DG: dentate gyrus; so: stratum oriens; sp: stratum pyramidalis; sr: stratum radiatum; calb: calbindin; MFI: mean fluorescence intensity.

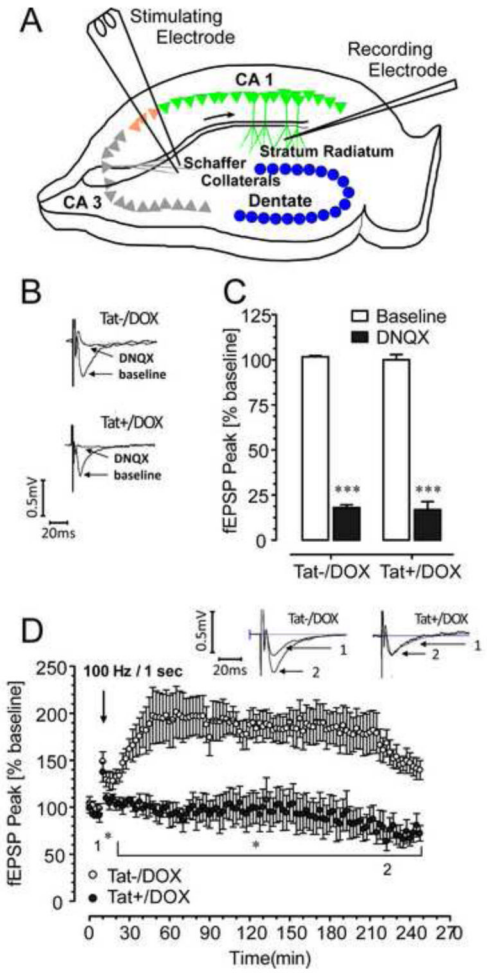

Figure 4.

Effects of Tat induction on synaptic transmission and synaptic plasticity. (A) Diagram of a transverse hippocampal slice, indicating the recording and stimulating electrode placements used to measure field excitatory postsynaptic potentials (fEPSP) in 1-mo old mice. (B) The amplitudes of the field potentials show representative traces for Tat−/DOX and Tat+/DOX mice before (control) and in the presence of 20 μM DNQX. (C) The average fEPSP peak data show a significant reduction of the fEPSP peak in the presence of DNQX. No significant difference was noted between the Tat−/DOX and Tat+/DOX mice for the baseline responses (control). (D) The fEPSP peak of LTP was significantly ($p < 0.01$) reduced in inducible (Tat+/DOX) mice (filled circles; $n = 4$) compared to control (Tat−/DOX) mice (open circles; $n = 4$). Insets show representative traces for both groups recorded before (indicated by 1) and 220 min after applying HFS (indicated by 2). The significant difference between LTP control and inducible mice is indicated in the graph (*$p < 0.05$ for the time period indicated by the bracket). HFS: high-frequency stimulation; *$p < 0.05$, ***$p < 0.001$; DOX: doxycycline.

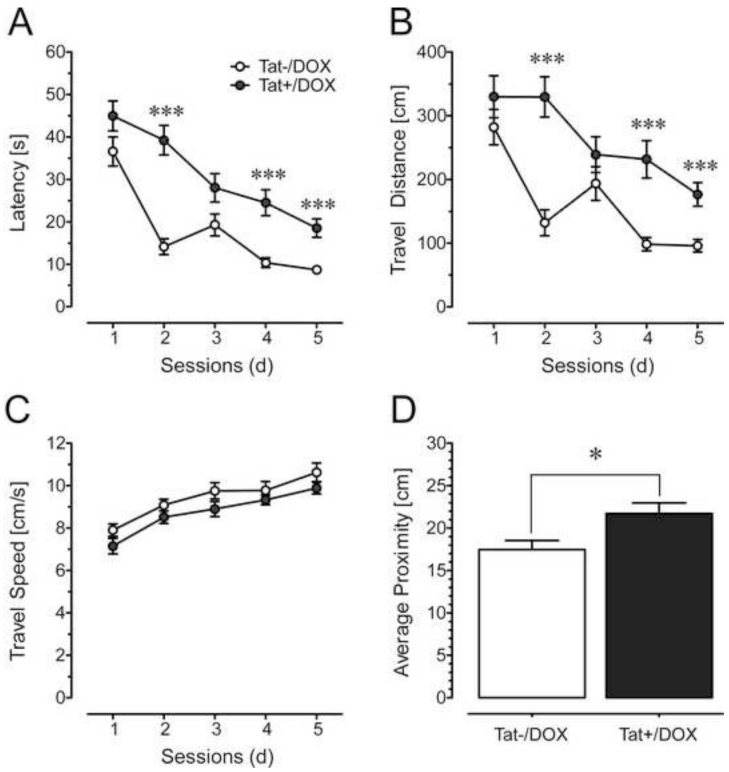

Figure 5.

Effects of Tat induction in the Morris water maze in acquisition training across session (A-C) and the probe test (D) for 2-3-mo old mice (mean ± SEM). (A-C) Two-way mixed ANOVAs were conducted with Tat induction as a between-subjects factor (2 levels) and session number (the data from 4 trials within each session were combined) as a within-subjects factor (5 levels). (A) Escape latency is increased for Tat+/DOX mice ($n = 9$) [main effect of Tat: $F(1, 16) = 49.47$, $p < 0.001$], indicating longer search times for Tat+/DOX mice to find the hidden platform compared to the control (Tat−/DOX, $n = 9$) mice. Post hoc tests conducted for each session reveal significant differences between the two groups for sessions 2, 4 and 5. There is also a learning effect across session for both groups expressed in a significant main effect of time [$F(4, 64) = 25.84$, $p_{GG} < 0.001$]. A Tat induction x session interaction [$F(4, 64) = 2.88$, $p_{GG} < 0.05$] indicates that with time, Tat−/DOX mice learn to find the hidden platform more rapidly than transgenic mice following Tat induction (Tat+/DOX). (B) Travel distance is increased for Tat+/DOX mice [main effect of Tat: $F(1, 16) = 36.02$, $p < 0.001$], with post hoc tests indicating that Tat+/DOX mice routinely swim longer distances before finding the platform for all sessions except at 3 d. There is also a learning effect across session for both groups [$F(4, 64) = 13.39$, $p_{GG} < 0.001$] as well as a significant Tat induction x session interaction [$F(4, 64) = 3.32$, $p_{GG} < 0.05$]. (C) Travel speed (cm/s) indicated a modest effect in the ANOVA for Tat induction [$F(1, 16) = 6.38$, $p < 0.05$] that however did not hold up in post hoc tests. Further, a significant session effect was noted, with both groups swimming faster across session [$F(4, 64) = 14.26$, $p_{GG} < 0.001$]. No Tat induction x session interaction was noted. (D) For the probe test, conducted 2 d after the last acquisition session, a one-way ANOVA was conducted with Tat induction as a between-subjects factor (2 levels). The proximity index (cm) indicated that control mice swim more closely to the previous location of the platform compared to the Tat+/DOX mice [Tat induction effect: $F(1, 15) = 6.54$, $p < 0.05$]. ***$p < 0.001$, *$p < 0.05$; DOX: doxycycline.

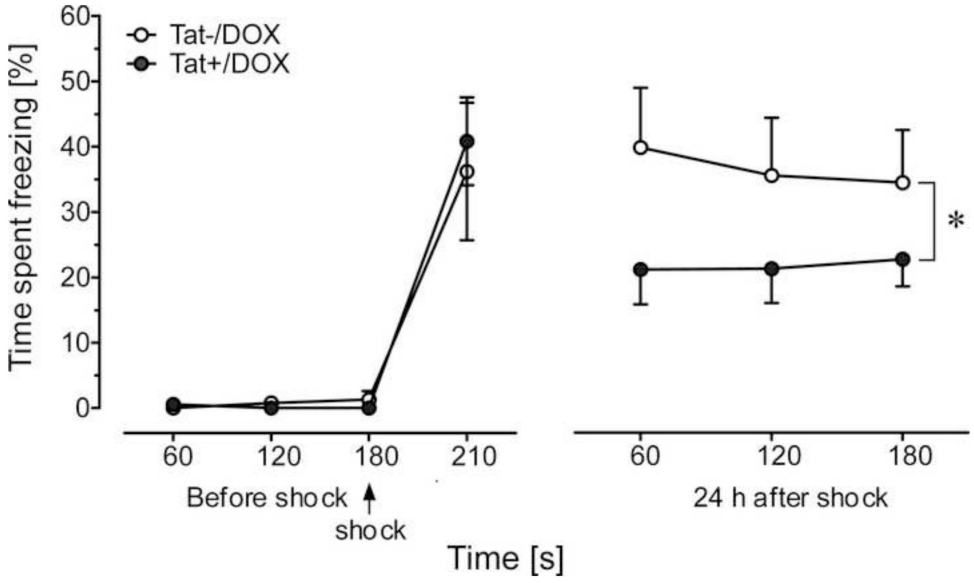

Figure 6.

Effect of Tat induction on contextual fear-conditioning assessments. No differences were observed in the freezing behavior of Tat−/DOX and Tat+/DOX mice either before or immediately after a conditioning foot shock (indicated by arrow, 3 min after baseline measures). However, there was a significant decrease in freezing behavior observed in mice expressing Tat protein (Tat+/DOX, $n = 9$) 24 h after foot shock conditioning, as compared to control Tat−/DOX [$n = 7$; main effect of group: $F(2,42) = 7.44$, $^{*}p < 0.01$] group. Data are mean ± SEM. DOX: doxycycline.

Table 1

Percent of viable neurons as estimated by TUNEL detection ($NeuN^+/TUNEL^-$) in the CA1 pyramidal neuronal layer.

	Tat−/DOX	Tat+/DOX	*p*-value
Neurons (% TUNEL−)	99.82 ± 0.14 (*n* = 4)	99.91 ± 0.06 (*n* = 4)	n.s.

Note: Data are mean ± SEM; n.s. = not significant.